Improvement of structural and superconducting properties of Bi-2212 textured rods by substituting sodium

O. Nane*[a], B. Özçelik[b], A. Sotelo[c], M. A. Madre[c]

[a] Department of Material Science and Engineering, Faculty of Engineering, Hakkari University, 30000 Hakkari, Turkey

[b] Department of Physics, Faculty of Sciences and Letters, Çukurova University. 01330 Adana, Turkey

[c] ICMA (CSIC-Universidad de Zaragoza). María de Luna, 3. 50018 Zaragoza, Spain.

Abstract

In this study, the physical and superconducting properties of $Bi_2Sr_2Ca_{1-x}Na_xCu_2O_{8+\delta}$ (x=0.0, 0.05, 0.075 0.1, and 0.20) textured superconducting rods prepared by a laser floating zone technique were presented. The effect of Na^{+1} substitution for Ca^{2+} has been investigated by X-ray diffraction, scanning electron microscopy, energy dispersive X-ray spectroscopy, transport measurements, dc-magnetization, magnetic hysteresis and magnetic critical current density. The powder XRD patterns of samples have shown that Bi-2212 phase is the major one, independently of Na content. Transport measurements indicate that, in general, the transport critical current density of samples is increased by Na substitution compared with the pure sample. In all cases, a good orientation of grains with the growth axis was observed in microstructural studies. The best critical temperature, T_C, was found as 93.3 K for the sample with 0.75Na substitution, under a DC magnetic field of 50 Oe in ZFC mode. It was also observed that the magnetic critical current density obtained from magnetic hysteresis curves by using the critical Bean's model, increases with increasing Na-substitution. The maximum magnetic J_C value was determined as 1.35×10^5 A/cm^2 at 10 K for the 0.10Na sample. The maximum transport critical current density was directly measured as 1.3×10^3 A/cm^2 at 77 K for the 0.05Na sample.

Keywords

Bi-2212, Sodium Substitution, Magnetic Properties, Critical Current Density J_C, Texturing, Laser Floating Zone Technique.

Introduction

The BSCCO family can be described by the $Bi_2Sr_2Ca_{n-1}Cu_nO_{2n+4+y}$ general formula, where n=1, 2, and 3. The n value indicates the number of CuO_2 layers in the crystal structure, producing the Bi-2201, Bi-2212 and Bi-2223 phases with critical temperatures, T_c's, of about 20, 85, and 110 K, respectively [1,2]. Among these phases, the Bi-2212 is stable in a wide range of compositions and processing temperatures but its Tc is greatly influenced by the chemical composition. Tc increases significantly when the Bi and Ca content is decreased, provided that the oxygen content is constant [3]. Since their discovery many experiments have been performed to better understand their structural and physical properties of the system, and to improve their critical temperature (Tc) and critical current density (Jc) [4-17], as it is considered as one of the most promising materials for technological applications. Besides, BSCCO superconductors have some advantages as high critical temperature and magnetic field carrying capacity, they also have some disadvantages like the weak-links, high anisotropy, and small coherence length. These restrict them for technological applications. Generally, even very small misorientation of grains in BSCCO superconductors produces a negative effect on Jc values. For many years, researchers have used many strategies in order to overcome those disadvantages and to maximize the transport properties at 77 K.

When BSCCO materials are properly textured, their transport properties are improved, in an important manner, compared with the non-textured materials. The Laser Floating Zone (LFZ) technique has been demonstrated to be an effective technique to produce a good grain orientation in Bi-2212 superconductors [18-22]. This method produces very high thermal gradients in the solidification front, producing a preferential alignment of grains with their c-axis perpendicular to the growth direction [23], maximizing the transport properties in the direction parallel to the growth axis.

In our previous works, the effect of sintering temperature on the Bi-(2212) phase formation, the optimum Na content to obtain the maximum amount of Bi-2212 phase and on the intergranular properties of polycrystalline $Bi_2Sr_2Ca_{1-x}Na_xCu_2O_{8+y}$ samples prepared by polymer method were studied [15,16,24]. Therefore, in this study, we have investigated the effects of Na^{+1} substitution for Ca^{+2} in Bi-2212 textured ceramics prepared by using the LFZ technique. X-ray diffraction, scanning electron microscopy, energy dispersive X-ray spectroscopy, transport measurements, dc-magnetization, magnetic hysteresis and magnetic critical current density were used to characterize the prepared samples.

Experimental

The initial $Bi_2Sr_2Ca_{1-x}Na_xCu_2O_x$ polycrystalline materials used in this work were prepared by a polymer solution method [25]. $Bi(CH_3COO)_3$ ($\geq$ 99.99 %, Aldrich), $Sr(CH_3COO)_2 \bullet 0.5H_2O$ (99 %, Panreac), $Ca(CH_3COO)_2 \bullet 2H_2O$ (98 %, Alfa Aesar), $Na(CH_3COO) \bullet 3H_2O$ ($\geq$ 99.99 %, Aldrich), and $Cu(CH_3COO)_2 \bullet H_2O$ (98 %, Panreac) commercial powders were used as starting materials. They were weighed in the appropriate proportions and dissolved in a mixture of distilled H_2O and glacial acetic acid (ACS Reagent, Panreac). Once a light clear blue solution has been obtained, polyethyleneimine (PEI, 50% aqueous, Aldrich) was added, turning it darker immediately due to the formation of metal cation-PEI complexes [26]. The solution was then introduced in a rotary evaporator where the volume was reduced to about 20 % of the initial one. The concentrated solution was subsequently placed onto a hot plate at about 75 ºC to totally evaporate the solvent, producing a thermoplastic royal blue paste [27]. Further heating at about 350 ºC produced the release of acetic acid-water vapours, followed by the release of brown fumes (CO_2, H_2O and NO_x) during the slow self combustion of organic material. The remaining brownish powder was manually milled and calcined at 750 and 800 ºC for 12 h with an intermediate manual milling to decompose the alkaline-earth carbonates. This step is very important for materials which are processed by the LFZ technique. If carbonates are present, they would decompose inside the molten zone, producing bubbles and destabilizing the crystallization front [28] leading to grain misorientations and parasitic grain growth. Moreover, some of the released CO_2 could be trapped inside the solid, producing porosity, and/or decreasing the grains connectivity.

The thermally treated powders were isostatically pressed in form of cylinders (between 2 and 3 mm diameter) at 200 MPa. The green ceramics were used as feed in in a directional solidification process performed in a LFZ installation [29]. The textured bars were obtained using a continuous power Nd:YAG laser (λ=1064 nm), under air, at a growth rate of 30 mm/h and 18 rpm relative rotation between seed and feed. After the melt-grown processes, very homogeneous geometrically bars were obtained ($\sim$ 2 mm diameter and 120 mm length). Bi-2212 ceramic presents incongruent melting and, as a consequence, after the directional solidification process, it is necessary to perform a thermal treatment in order to form the Bi-2212 superconducting phase [30]. This annealing process was performed under air, and consisted in two steps: 60 h at 860 ºC, followed by 12 h at 800 ºC and, finally, quenched in air to room temperature.

Structural studies of textured ceramic samples were performed by using a Rigaku D/max-B X-ray powder diffractometer (CuKα radiation) with 2θ ranging between 3 and 80 degrees.

The uncertainty of the crystal lattice parameters calculation remained in the ±0.00001 range. Microstructural features were determined on polished longitudinal cross-sections of samples, in a field emission scanning electron microscope (FESEM, Zeiss Merlin) equipped with an energy dispersive spectroscopy (EDX) system. The magnetic hysteresis measurements of samples were performed at temperature of 10 K and an applied field of ±1 T, and M(T) measurement obtained under applied fiel of 50 Oe in ZFC mode with a 7304 model Lake Shore VSM. Transport measurements were performed by conventional four-point probe configuration on about 30 mm long samples.

Results and Discussion

The powder XRD patterns for all samples are shown in Fig. 1. As can be seen, all peaks detected above %3 of the maximum intensity value and labeled by + are related to the major Bi-2212 phase. The unit-cell parameters and average crystal sizes calculated by using least square fitting and the Debye-Scherrer formula [31], respectively, are given in Table 1. The crystal symmetries of all samples are obtained as pseudo-tetragonal structure with a-b≈5.40 Å. The c-parameters of all samples are found in the vicinity of 30.8 Å, which is in good agreement with the crystal structure of Bi-2212 phase [32]. The crystal size indicating the crystallinity first increases with increasing of Na concentration up to 0.10Na and then it starts to decrease. As a consequence, an increasing of Na-concentration may help to the growth mechanism of Bi-2212 grains in grain boundaries. On the other hand, lower melting point of system arising from more concentration of Na induces a small amount of liquid phase in the grain boundaries. Those liquid phases contribute to diffusion mechanism that can help to growing of the grains.

Fig. 2 shows the SEM micrographs obtained from longitudinal polished sections of samples. As it can be seen, the SEM images have different contrasts indicating the different phases in the structures. It can be also clearly seen that Bi-2212 (grey phase indicated by #1) is the major phase observed in all samples. The phase marked as #2 (white contrast) are identified as Bi-2201 phase. Finally, black spots marked as #3 correspond to strontium rich phase. It is observed that all samples are formed of well-textured grain structure of typical Bi-2212 superconductor phase. In addition, the sample having 0.075Na contains less Bi-2201 phase (white color) those of the others. Therefore, it may positively contribute to transport properties and superconducting transition temperature, T_C, of this sample.

Fig. 3 shows the magnetizations as a function of temperature measured under applied magnetic field of 50 Oe, perpendicular to the growth direction of fibers. As can be seen from the inset figure, the critical onset temperatures, T_C, corresponding to diamagnetic transition are evaluated to be around 92 K with a sharp drop for all samples indicating a good quality, homogeneity, and texturing of the fibers. The T_C values slowly vary depending on the Na-concentration. Initially, it increases with increasing Na-concentration up to 0.1Na substitution for Ca, and then it decreases with increasing Na-concentration. The best T_C value is obtained as 93.3 K for the sample having %7.5 of Na, which is also very close to superconducting transition temperature value of single crystal of Bi-2212 phase [33]. This result is compatible with its SEM micrograph demonstrating less fraction of Bi-2201 phase, larger well oriented grain structure of Bi-2212.

Figure 4 illustrates the magnetic hysteresis loops measured at 10 K, between the applied magnetic fields of ±9 T, perpendicular to the growth direction. The general behavior of hysteresis curves appeared in the figure indicates that the magnetization values are strongly dependent to Na-substitution. Furthermore, the reversible and symmetrical shapes of loops imply that pinning mechanism commonly occurs by bulk pinning rather than surface and geometrical barriers in low fields [34]. As it can be seen, the M-H loops of 10%, 15% and 5% are relatively larger than those of pure sample. A large hysteresis loop and high magnetization value lead to a high intra-grain critical current density value. It is concluded that diamagnetic response may be firstly affected positively up to 10% of Na-substitution level, than it starts to be negatively affected by rising of Na content.

The intragranular critical current density Jc, values of the samples were calculated from the hysteresis data measured at 10 K, using the Bean's model [35].

$$Jc = 30\frac{\Delta M}{d}$$

where J_C is the critical current density in ampéres per square centimeter of a sample. $\Delta M = M_+ - M_-$ is measured in electromagnetic units per cubic centimeter, and d is the thickness of the sample.

Figure 5 shows intragranular critical current densities for all samples, as a function of applied magnetic field, at 10 K.

It is observed that Jc^{mag} values gradually decrease with increasing magnetic field values. It can be also seen that Na substitution for Ca site of Bi-2212 system generally contributes to the pinning mechanism. The reason may be explained by using SEM micrographs of fibers composing of well-textured grain orientations induced by Na-content. A larger and textured grain implies strong grain boundaries revealing to the high J_C^{mag} values. The sample having 10 percentage of Na-substitution exhibits the highest J_C^{mag} value. It is found as 1.33×10^5 A/cm^2 at 10 K in the absence of magnetic field.

We have also measured directly the critical current values of the samples. Figure 6 shows intergrain critical current density, J_C, versus Na-substitution level at 77 K. In this figure, it seems that the transport J_C values of all Na-substituted samples are relatively higher than the pure sample, due to better texturing and larger grain size. The best J_C value was obtained as 1.3×10^3 A/cm^2 at 77 K for x=0.05. There is a local minimum for Na-substituted samples at x=0.1, than J_C increase gradually for more Na concentration.

Conclusion

In this study, the effect of Na substitution for Ca on the structural and superconducting properties of Bi-2212 prepared by polymer solution method and then directionally grown using the laser floating zone (LFZ) technique has been investigated. XRD measurements suggest that all fiber samples have grown with nearly single Bi-2212 phase independently from Na-substitution. The SEM micrographs and EDX results of all samples indicate that Bi-2212 is major phase with a rarely appearance of Bi-2201 phase and phase rich in Sr. According to *M-T* results, Na-substitution results an improvement in superconducting transition temperature T_C, as about 1K for x=0.075. The *M-H* measurements indicate that the hysteresis loops relatively become larger for x= 0.05, 0.1, and 0.15 with texturing process. The critical current density is improved for some Na-substitution levels, implying well textured and larger grain clusters compared with the pure fiber sample. The highest intragranular J_C^{mag} value was calculated as 1.33×10^5 A/cm^2 at 10 K for x=0.1, while the highest intergranular J_C was measured as 1.3×10^3 A/cm^2 at 77 K for x=0.05.

References

[1] C. Michel, M. Hervieu, M.M. Borel, A. Grandin, F. Deslands, J. Provost, B. Raveav, Superconductivity in the Bi-Sr-Cu-O System, Z. Phys. B 86, 421 (1987)

[2] H. Maeda, Y. Tanaka, M. Fukutumi, T. Asano, A new high-Tc oxide superconductor without a rare-earth element, Jpn. J. Appl. Phys. 27, 209 (1988)

[3] P. Majewski, H. L. Su, M. Quilitz, Relationships between the chemical composition and properties of the high-temperature superconductor $Bi_{2+x} Sr_{2-y}Ca_{1+y} Cu_2O_{8+d}$, J. Mater. Sci. 32, 5137 (1997)

[4] N. Türk, H. Gündogmus, M. Akyol, Z. D. Yakıncı, A. Ekicibil, B. Özçelik, Effect of Tungsten (W) Substitution on the Physical Properties of Bi-(2223) Superconductors, J Supercond Nov Magn27, 711 (2014)

[5] V. Lennikov, B. Özkurt, L. A. Angurel, A. Sotelo, B. Özçelik, G. F. de la Fuente, Microstructure and Transport Properties of Bi-2212 Prepared by CO2 Laser Line Scanning, J Supercond.Nov.Magn. 26, 947, (2013)

[6] B. Özçelik, B. Özkurt, M.E. Yakıncı, A. Sotelo, M. A. Madre, Relationship Between Annealing Time and Magnetic Properties in Bi-2212 Textured Composites,J Supercond Nov Magn. 26:873 (2013)

[7] D. Yazıcı, B. Ozçelik, M.E. Yakıncı, Improvement of High Tc Phase Formation in BPSCCO Superconductor by Adding Vanadium and Substituting Titanium,J. Low Temp. Phys. 163, 370 (2011)

[8] A. Sotelo, M. Mora, M. A. Madre, J. C. Diez, L. A. Angurel, G. F. de la Fuente, Ag distribution in thick Bi-2212 floating zone textured rods, J. Eur. Ceram. Soc. 25, 2947 (2005)

[9] A. Sotelo, P. Majewski, H. S. Park, F. Aldinger, Synthesis of highly pure Bi-2223 ceramics using defined precursors, Physica C 272, 115 (1996)

[10] M. Mora, A. Sotelo, H. Amaveda, M. A. Madre, J. C. Diez, L. A. Angurel, G. F. de la Fuente, Ag addition effect on laser textured Bi-2212 samples, Bol. Soc. Esp. Ceram. V. 44, 199 (2005)

[11] G. F. de la Fuente, A. Sotelo, Y. Huang, M. T. Ruiz, A. Badia, L. A. Angurel, F. Lera, R. Navarro, C. Rillo, R. Ibañez, D. Beltran, F. Sapiña, A. Beltran, Polymersolution processing of (Bi,Pb)-Sr-Ca-Cu-O, Physica C185, 509 (1991)

[12] S. Bal, M. Dogruer, G. Yıldırım, A. Varilci, C. Terzioglu, Y. Zalaoglu, Role of Cerium Addition on Structural and Superconducting Properties of Bi-2212 System, J. Supercond. Nov. Magn. 25, 847 (2012)

[13] B.Ozkurt, Enhancement in superconducting transition temperature and Jc values in Na-doped $Bi_2Sr_2Ca_1Cu_{2-x}Na_xO_y$ superconductors, J Mater Sci: Mater Electron., 24, 2426 (2013)

[14] B. Özçelik, M.Gürsul, A. Sotelo, M. A. Madre, Effect of K substitution on Structural, Electrical and Magnetic Properties of Bi-2212 system, J. Mater. Sci.: Mater. Electron. 25, 4476 (2014)

[15] B. Özçelik, M.Gürsul, A. Sotelo, M. A. Madre, Improvement of superconducting properties in Na-doped BSCCO superconductor, J. Mater. Sci.: Mater. Electron. 26, 441 (2015)

[16] B. Özçelik, M.Gürsul, A. Sotelo, M. A. Madre, Improvement of the intergranular pinning energy in the Na-doped Bi-2212 superconductors, J. Mater. Sci.: Mater. Electron. 26, 2830 (2015)

[17] B. Özçelik, E.Yalaz, M.E.Yakıncı, A. Sotelo, M. A. Madre, The Effect of K Substitution on Magnetoresistivity and Activation Energy of Bi-2212 System, J. Mater. Sci.: Mater. Electron. 28, 553 (2015)

[18] B. Özkurt, M. A. Madre, A. Sotelo, M.E. Yakıncı, B. Özçelik, Relationship Between Growth Speed, Microstructure, Mechanical and Electrical Properties in Bi-2212/Ag Textured Composites, J. Supercond. Nov. Magn. 25, 799 (2012)

[19] H.Gündoğmuş, B. Özçelik, A. Sotelo, M. A. Madre, Effect of Yb-substitution on thermally activated flux creep in the Bi2Sr2CaCu2-xYbxOy superconductors,J Mater Sci: Mater Electron 24, 2568 (2013)

[20] A. Özaslan, B. Özçelik, B. Özkurt, A. Sotelo,M.A. Madre, Structural, Electrical, and Magnetic Properties of the Co-Substituted Bi-2212 System Textured by Laser Floating Zone Technique, J Supercond Nov Magn 27, 53 (2014)

[21] B. Özçelik, C. Kaya, H. Gündoğmuş, A. Sotelo, M.A. Madre, Effect of Ce Substitution on the Magnetoresistivity and Flux Pinning Energy of the Bi2Sr2Ca1-xCexCu2O8+d Superconductors, J Low Temp Phys. 174, 136 (2014)

[22] A. Sotelo, M. Mora, H. Amaveda, J. C. Diez, L. A. Angurel, M. C. Mayoral, Study of the variation of the E-I curves in the superconducting to normal transition of Bi-2212 textured ceramics by Pb addition, Bol. Soc. Esp. Ceram. V. 45, 228 (2006)

[23] G. F. de la Fuente, M.T. Ruiz, A. Sotelo, A. Larrea, R. Navarro, Microstructure of laser floating zone (LFZ) textured (Bi, Pb)-Sr-Ca-Cu-O superconductor composites, Mater. Sci. Eng. A 173, 201 (1993)

[24] M.Gürsul, A. Ekicibil, B. Özçelik, M. A. Madre, A. Sotelo, Sintering Effects in Na-Substituted Bi-(2212) Superconductor Prepared by a Polymer Method, J Supercond Nov Magn 28, 1913 (2015)

[25] B. Özçelik, M.Gürsul, A. Sotelo, M. A. Madre, Improvement of the intergranular pinning energy in the Na-doped Bi-2212 superconductors, J. Mater. Sci.: Mater. Electron. 26, 2830 (2015)

[26] H. Gundogmus, B. Ozcelik, B. Ozkurt, A. Sotelo, M.A. Madre, Physical, mechanical and magnetic properties of the Yb substituted Bi2Sr2Ca1Cu2Oy textured superconductor J. Supercond. Nov. Magn. 26, 111 (2013)

[27] A. Sotelo, G. F. de la Fuente, F. Lera, D. Beltran, F. Sapiña, R. Ibañez, A. Beltran, M. R. Bermejo, Novel polymer solution synthesis of the 110 K superconducting phase in the bismuth system, Chem. Mater. 5, 851-856 (1993)

[28] A. Sotelo, Sh. Rasekh, M. A. Madre, J. C. Diez, Precursor Influence on the Electrical Properties of Textured Bi-2212 Superconductors, J. Supercond. Nov. Magn. 24, 19 (2011)

[29] M. F. Carrasco, F. M. Costa, R. F. Silva, F. Gimeno, A. Sotelo, M. Mora, J. C. Diez, L. A. Angurel, Textured BI-Sr-Ca-Cu-O rods processed by laser floating zone from solid state or melted precursors, Physica C 415, 163 (2004)

[30] M. Mora, A. Sotelo, H. Amaveda, M. A. Madre, J. C. Diez, F. Capel, J. M. Lopez-Cepero, Properties variation of Bi-2212 directionally solidified induced by 0.4Pb substitution, J. Eur. Ceram. Soc. 27, 3959 (2007)

[31] P. Scherrer, Bestimmung der Größe und der inneren Struktur von Kolloidteilchen mittels Röntgenstrahlen, Göttinger Nachrichten Gesell 2 (1918)

[32] X. Zhao, W. Wu, X. Sun, X.G. Li, New experimental evidence of the structural modification in single crystal Bi Sr CaCu O by X-ray diffraction observation, Physica C 320, 225 (1999)

[33] Eisaki H, Kaneko N, Feng D L, Damascelli A, Mang P K, Shen K M, Shen Z X and Greven M, Effect of chemical inhomogeneity in bismuth-based copper oxide superconductors, Phys. Rev. B 69, 064512 (2004)

[34] B. Özkurt, A. Ekicibil, M. Ali Aksan, B. Özçelik, M. E. Yakıncı,K. Kiymaç, Structural and Physical Properties of Nd Substituted Bismuth Cuprates $Bi_{1.7}Pb_{0.3-x}Nd_xSr_2Ca_3Cu_4O_{12+y}$, J. Low Temp Phys, 149, 105 (2007)

[35] C.P. Bean, Magnetization of Hard Superconductors, Phys. Rev. Lett. 8, 250 (1962)

Figure Captions

Figure-1. XRD patterns of the samples which are milled. Peaks are indicated by + corresponding to the Bi-2212.

Figure-2. SEM micrographs performed on longitudinal polished sections of the samples.

Figure-3. Magnetic moment as a function of temperature for different Na-concentrations.

Figure-4. Magnetic Hysteresis curves obtained for the all samples at 10 K.

Figure-5. Calculated critical current densities, *Jc*, of the samples, as a function of applied field at 10 K.

Figure-6. Critical current density *Jc*, at 77K, vs. Na concentration for Bi-2212 Fibers.

Table

Table-1. T_C values determined from M-T measurement, unit-cell parameters, crystal size, and J_C values for all concentration.
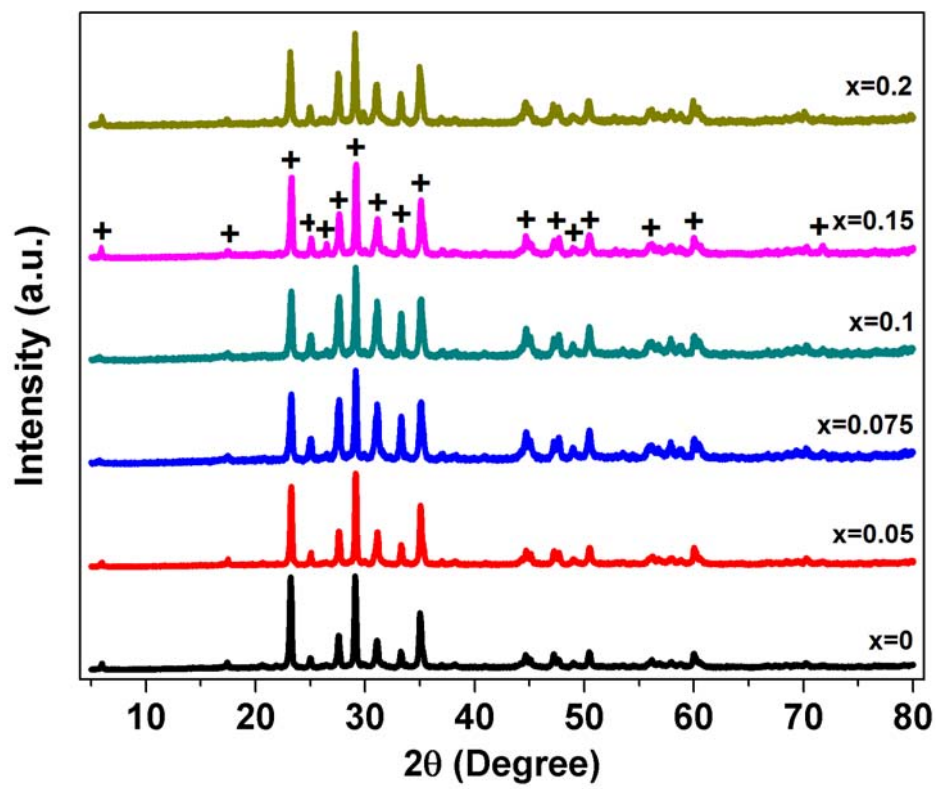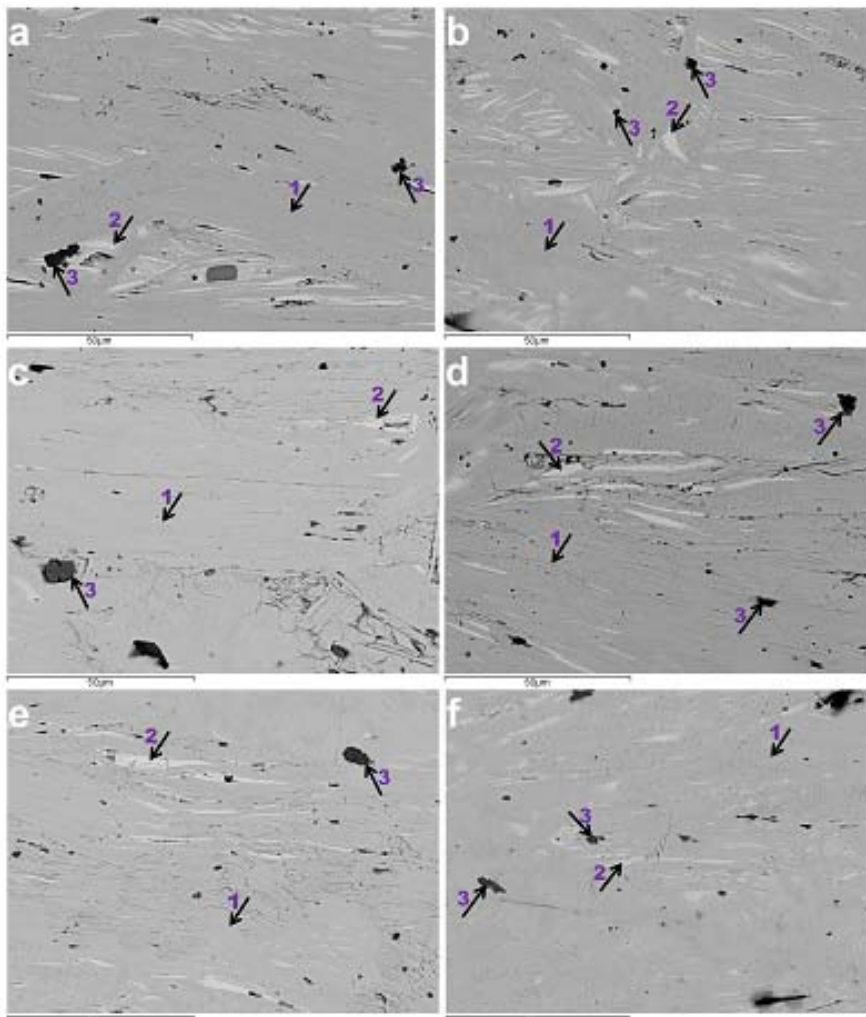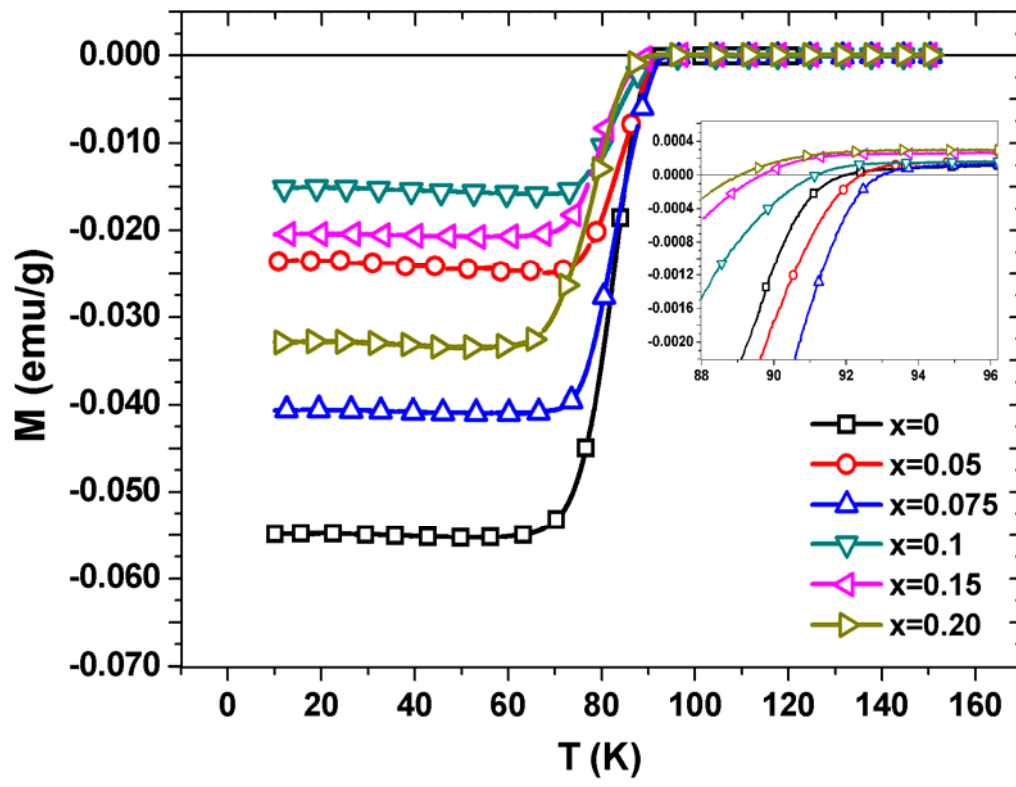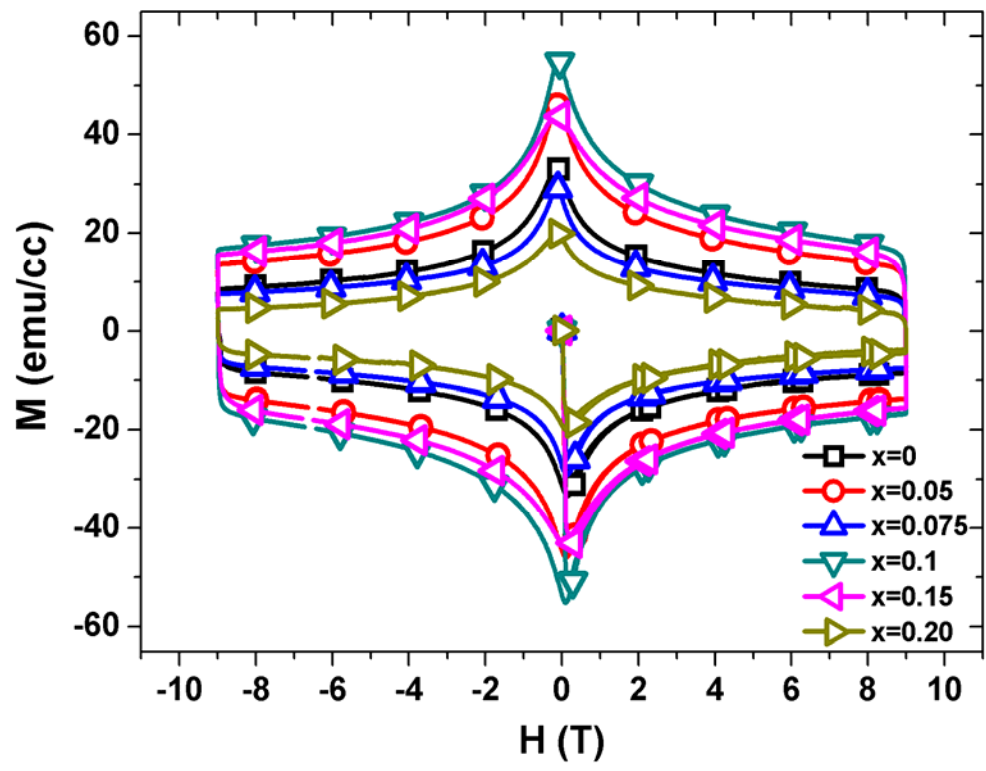
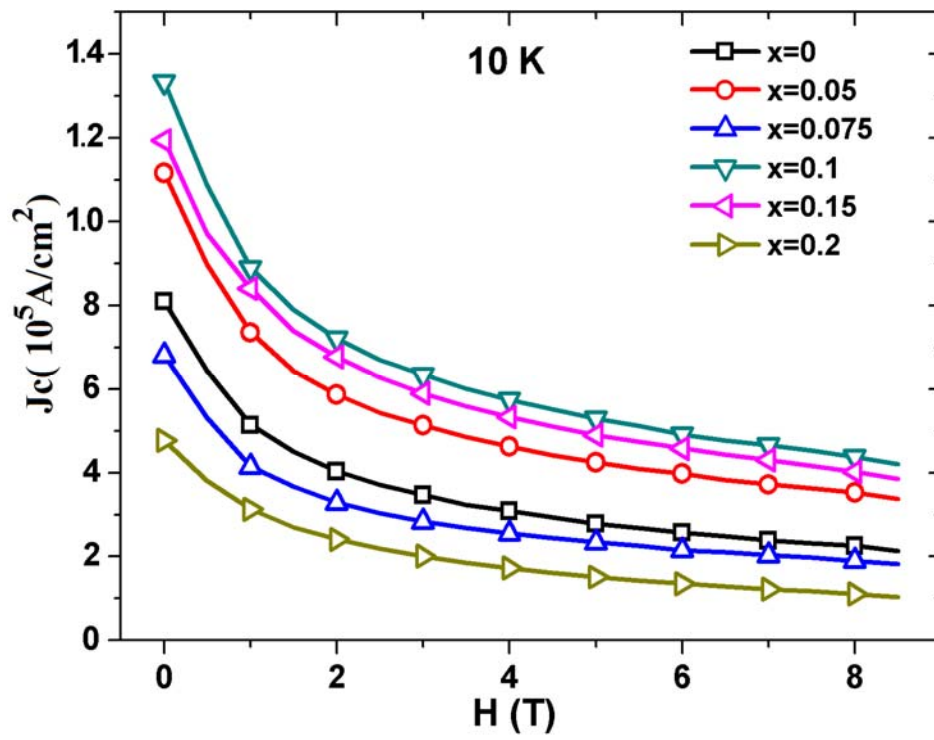**Fig.1.**

Fig.2.

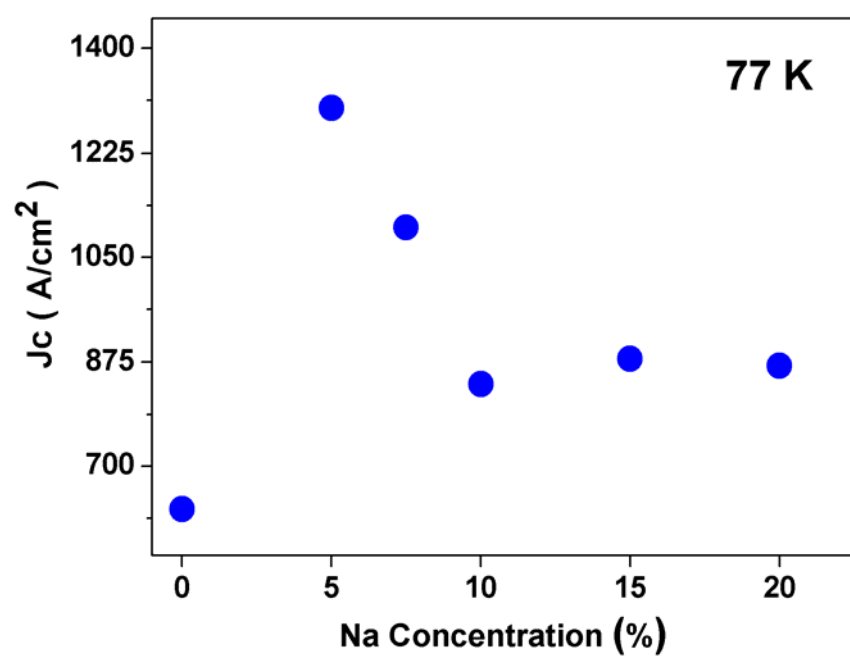**Fig.3.**

Fig.4.

Fig.5.

Fig.6.

Na-Content	T_C (K)	Unit-cell Parameter $a \approx b$ (Å)	Unit-cell Parameter c	Crystal Size L (Å)	Intragranular J_C (A/cm^2) at 10 K	Intergranular J_C (A/cm^2) at 77 K
x=0	92.5	5.4212	30.8945	430.12	0.81×10^5	0.63×10^3
x=0.05	92.6	5.4457	30.9106	442.88	1.11×10^5	1.30×10^3
x=0.075	93.3	5.4305	30.8382	444.86	0.68×10^5	1.10×10^3
x=0.1	91.4	5.4289	30.9439	488.47	1.33×10^5	0.84×10^3
x=0.15	89.9	5.4211	30.8998	416.94	1.19×10^5	0.88×10^3
x=0.2	89.3	5.4243	30.9107	410.07	0.47×10^5	0.87×10^3

Table-1.